J. Plasma Physics (1998), *vol.* 59, *part* 1, *pp.* 179–191. Printed in the United Kingdom
© 1998 Cambridge University Press

Envelope nonlinear drift structures in a non-equilibrium plasma near the boundary of marginal stability

TATIANA A. DAVYDOVA and ALEXEI YU. PANKIN
Plasma Theory Department, Institute for Nuclear Research,
pr. Nauki, 47, Kiev – 252022, Ukraine

(Received 23 May 1997 and in revised form 1 July 1997)

An explosive instability of the ion-temperature-gradient (ITG)-driven modes (η_i modes) near the boundary of marginal stability is considered as a driving mechanism for subcritical turbulence. It is shown that boundedness of the wave interaction region leads to saturation of the instability. The possibility of coherent soliton-like structure formation in both slab and toroidal geometries is demonstrated by numerical simulation. An analytical soliton solution is found in some special cases.

1. Introduction

The formation of coherent long-lived large-scale structures of drift modes is sometimes considered to be one of the main reason for L–H transition to the regime of improved confinement in tokamaks (Ottaviani *et al.* 1990) and sometimes as the reason for anomalous transport (Horton *et al.* 1990; Pavlenko and Weiland 1993). Although the connection between anomalous transport and coherent structures is still unclear, recent experiments indicate that the correlation length that determines the local transport is determined by nonlinear effects (Weiland 1994). Recently Riccardi *et al.* (1996) have obtained new experimental evidence that nonlinear wave–wave interaction between spontaneously excited quasicoherent drift modes can lead to turbulence in a toroidal plasma. The ion-temperature-gradient (ITG)-driven modes along with the trapped-electron mode and the pressure-gradient ballooning modes are the dominant instabilities for the most realistic tokamak parameters (low β and weak collisionality), and in many cases are responsible for ion anomalous transport in tokamak plasmas (Connor 1995). The ITG-driven mode (or η_i mode) is driven by ion temperature gradients and is characterized by parameters $\eta_i = d\ln T/d\ln n$ and $\varepsilon_n = 2d\ln B/d\ln n$. A critical value of the parameter η_{icr} determines the threshold below which the mode is linearly stable (Nordman and Weiland 1989). Much experimental evidence (Romanelli *et al.* 1986; Kurki-Suonio *et al.* 1992) indicates that the tokamak plasma profiles are in line with the assumption that the plasma is near the boundary of marginal stability for the η_i mode. Some kinetic simulations show also that the ITG-driven mode is often close to the linear stability boundary for measured tokamak parameters (Rewoldt *et al.* 1987). These results agree with the profile consistency principle that was proposed by Coppi (1980), and supported later by Terry *et al.* (1988) and Kishimoto *et al.* (1996). One of the approaches to anomalous transport is that the increased

https://doi.org/10.1017/S0022377897006193 Published online by Cambridge University Press

transport will bring the density $n(r)$ and temperature $T(r)$ profiles in tokamak plasmas to marginal stability of strong reactive unstable modes such as the ITG-driven modes. This could be considered as support for the idea of self-organization of tokamak plasmas. Below the linear stability boundary, there still exists a rather high level of turbulence – so called 'subcritical turbulence'. This is true not only for reactive drift modes like ITG-driven modes. Subcritical turbulence has also been observed in fluid dynamics (Dauchot and Daviaud 1995) and in MHD plasmas (Walts 1985).

Close to the stability boundary, the system behaviour changes essentially, and requires special analytical treatment. Nordman *et al.* (1993) have proposed the nonlinear explosive instability due to the interaction between modes with positive and negative energy as the driving mechanism for the subcritical turbulence. As shown by Davydova *et al.* (1976) the character of nonlinear wave interaction radically changes near the stability boundary. When all interacting modes are 'zero-energy modes' the characteristic nonlinear interaction time t_0 is the least (Davydova 1982; Moiseev *et. al.* 1983; Davydova *et al.* 1987). By 'zero-energy wave' we mean a quasi-monochromatic wave of frequency ω_k for which the following conditions hold:

$$\omega_k^{-1} \ll \tau_{nl} \ll \left| \frac{1}{E(\omega_k)} \left[\frac{dE(\omega)}{d\omega} \right]_{\omega=\omega_k} \right|, \tag{1.1}$$

where τ_{nl} is the characteristic time of the nonlinear process and $E(\omega)$ is the energy of the quasimonochromatic wave, $E(\omega_k) = A^2 \omega_k [\partial D/\partial \omega]_{\omega=\omega_k}$, $D(\omega, k) = 0$ is the linear dispersion equation, and A is the wave amplitude. The inequalities (1.1) are consistent for a sufficiently large wave amplitude near the stability boundary of a wave with frequency $\omega_k (D(\omega_k, k) = 0, [\partial D/\partial \omega]_{\omega=\omega_k} = 0)$. Then mode-energy exchange during nonlinear interaction greatly exceeds the modes' 'own' energies. Another important feature of nonlinear wave interaction near the stability boundary is that the possibility of explosive instability does not depend on the signs of the modes' 'own' energies or on the signs of the interaction-matrix elements if two or three waves from a resonant triad are 'zero-energy waves' (Davydova and Zmudskii 1994).

The purpose of this paper is to investigate nonlinear explosive instabilities of η_i modes near the boundary of marginal stability and their possible saturation mechanisms. A number of saturation mechanisms of explosive instabilities are known. If the free energy is kept unaltered at the expense of the energy of external sources then self-stabilization of the wave–wave interaction by a nonlinear frequency shift (in the second order of perturbation theory) is possible (Davydova 1984). Higher-order nonlinear effects restrict the increase of interacting wave amplitudes at rather high amplitudes. Boundedness of the wave interaction region due either to the inhomogeneity of the medium, leading to detuning of the wave phases, or to the boundedness of the system may affect the explosive instability dynamics. In this case the explosive instability is saturated at sufficiently low wave amplitudes if unstable perturbations escape from the interaction region in a time small compared with the 'explosion time'. The stabilization conditions for the usual explosive instability due to inhomogeneity of the medium have been found by Davydova and Oraevskii (1974). Below some wave intensity threshold, only finite spatial wave amplification takes place. This conclusion was applied by Mordovskaya and Oraevskii (1985) to explain the formation of small-scale structures

https://doi.org/10.1017/S0022377897006193 Published online by Cambridge University Press

in the auroral plasma. In the case of modified explosive instability (1.1) frequency mismatch in an inhomogeneous medium gives a threshold for instability only if the signs of the matrix elements are equal (Davydova and Zmudskii 1994). For different signs of the matrix elements, temporal 'explosion' of 'zero-energy waves' does not stop in the first order of perturbation theory (Davydova and Zmudskii 1994). We show here that taking account of the finite size of the interaction region implies that the instability threshold exists for any signs of the matrix elements.

The paper is organized as follows. In Sec. 2 we outline a hydrodynamic slab model of η_i modes near the boundary of marginal stability. In Sec. 3 we review briefly the time development of the modified explosive instability of three resonantly coupling η_i modes, and in Sec. 4 we show how the development is modified on accounting for a finite size of the interaction region. We demonstrate analytically and numerically that in a bounded region of extent L the evolution of explosive instability of ITG-driven modes near the boundary of marginal stability may lead to a steady state if L is less than the 'explosive' length for any signs of the matrix elements. A finite interaction region of interacting wave packets is created in the self-organized process during spatial temporal instability evolution. This process may lead to drift-wave envelope nonlinear structure (soliton) formation. In Sec. 5 we find particular analytical solutions in the form of solitons, and confirm numerically the existence of soliton solutions in cases of homogeneous as well as inhomogeneous background parameters. Section 6 contains a discussion of our results.

2. Basic equations

A wide range of theoretical descriptions of the η_i mode have been given in the last few decades. The main treatments are local (Biglary *et al.* 1989; Romanelli 1989) and non-local (Romanelli and Zonca 1993; Taylor *et al.* 1996) approximations, and fluid (Nordman and Weiland 1989; Shukla and Weiland 1989; Horton *et al.* 1981; Andersson and Weiland 1988) and kinetic (Romanelli 1989; Guzdar *et al.* 1983; Hahm and Tang 1989) descriptions, in slab (Nordman and Weiland 1989; Andersson and Weiland 1988; Hahm and Tang 1989) and toroidal (Romanelli and Zonca 1993; Taylor *et al.* 1996) geometry. We explore here a reactive slab fluid model in the electrostatic approximation (Nordman and Weiland 1989; Andersson and Weiland 1988). The basic set of equations consists of the ion continuity equation and the ion momentum and energy equations. Compared with earlier fluid models (Horton *et al.* 1981), the present model combines simplicity with a satisfactory description that is in an agreement with the results of the kinetic model. The model takes into account all inhomogeneities (density, temperature and magnetic field) in the radial ($\widehat{\boldsymbol{x}}$) direction, finite-Larmor-radius effects and the difference between the ion and electron temperatures. For simplicity, we put here $\tau = T_e/T_i = 1$. Then, in a Fourier representation, the model equations take the forms

$$\left(i\frac{\partial}{\partial t} + k_y A\right) T_k + k_y B \Phi_k = i \sum_{k_1,k_2} (X^{(1)}_{k k_1 k_2} \Phi^*_{k_1} \Phi^*_{k_2} + Y^{(1)}_{k k_1 k_2} T^*_{k_1} \Phi^*_{k_2}), \qquad (2.1a)$$

$$\left(i\frac{\partial}{\partial t} + k_y C\right) \Phi_k + k_y D T_k = i \sum_{k_1,k_2} (X^{(2)}_{k k_1 k_2} \Phi^*_{k_1} \Phi^*_{k_2} + Y^{(2)}_{k k_1 k_2} T^*_{k_1} \Phi^*_{k_2}), \qquad (2.1b)$$

https://doi.org/10.1017/S0022377897006193 Published online by Cambridge University Press

where T_{k_j} and Φ_{k_j} are the Fourier components of the ion temperature and the electrostatic potential perturbations, which are normalized as follows:

$$\widehat{T} = \frac{L_n}{\rho_s}\frac{\delta T}{T}, \quad \widehat{\Phi} = \frac{L_n}{\rho_s}\frac{e\Phi}{T}, \quad T = T_e = T_i.$$

The matrix elements $X^{(1)}_{kk_1k_2}$, $X^{(2)}_{kk_1k_2}$, $Y^{(1)}_{kk_1k_2}$ and $Y^{(2)}_{kk_1k_2}$ are given by Nordman *et al.* (1993). The dimensionless time and space coordinate are

$$t \to \omega_s t, \quad \overline{r} \to \frac{\overline{r}}{\rho_s}.$$

Here we have used the notation

$$\begin{aligned}
A &= \tfrac{1}{3}\varepsilon_n(7 - 2k^2),\\
B &= \tfrac{4}{3}\varepsilon_n(1 - k^2) - \eta_i + \tfrac{2}{3}(2 + \eta_i)k^2,\\
C &= \varepsilon_n(1 - k^2),\\
D &= 2C - \frac{1 - (1 + \eta_i)k^2}{1 + k^2},\\
\omega_s &= \frac{c_s}{L_n}, \quad \rho_s = \frac{c_s}{\Omega_{ci}}, \quad L_n = \frac{d\ln n}{dx}.
\end{aligned}$$

In the linear approximation, one can put $\Phi_{k_j}, T_{k_j} \propto \exp(-i\omega_{k_j}t)$ and obtain the linear dispersion relation for η_i modes:

$$\begin{aligned}
\omega^{\pm}_{k_j} &= \tfrac{1}{2}k_{yj}\,(A + D) \pm \tfrac{1}{2}k_{yj}[(A - D)^2 + 4BC]^{1/2}\\
&= \tfrac{1}{2}k_{yj}(1 - \tfrac{13}{3}\varepsilon_n) - \tfrac{3}{8}k^2_{yj}\,(\varepsilon_n + \eta_i) \pm \tfrac{1}{2}k_{yj}\delta_k,
\end{aligned} \tag{2.2}$$

where

$$\begin{aligned}
\delta_j &= 2\left[\varepsilon_n\left(\eta_{icr} - \eta_i\right)\right]^{1/2},\\
\eta_{icr} &= \eta^0_{icr} + k^2\left[2 - \frac{5}{18}\varepsilon_n - \frac{1}{2\varepsilon_n} - \frac{\eta^0_{icr}}{2}\left(1 + \frac{1}{\varepsilon_n}\right)\right],\\
\eta^0_{icr} &= \frac{1}{6} + \frac{49}{36}\varepsilon_n + \frac{1}{4\varepsilon_n}.
\end{aligned}$$

For weak nonlinearities ($\tau_{nl} \gg \omega_k^{-1}$), the basic set of equations for the amplitudes of three resonantly interacting waves for which

$$\omega_{k_1} + \omega_{k_2} + \omega_{k_3} = 0, \quad \boldsymbol{k}_1 + \boldsymbol{k}_2 + \boldsymbol{k}_3 = 0, \tag{2.3}$$

reduces to the set of three equations

$$\widehat{L}_1\Phi_2 = V_{k_1k_2k_3}\Phi^*_2\Phi^*_3, \tag{2.4a}$$

$$\widehat{L}_2\Phi_3 = V_{k_2k_3k_1}\Phi^*_1\Phi^*_3, \tag{2.4b}$$

$$\widehat{L}_3\Phi_3 = V_{k_3k_1k_2}\Phi^*_1\Phi^*_2, \tag{2.4c}$$

where

$$\begin{aligned}
\widehat{L}_j = {} & \pm ik_{yj}\delta_j\left(\frac{\partial}{\partial t} - u_j\frac{\partial}{\partial y}\right) + \left(\frac{\partial}{\partial t} - u_j\frac{\partial}{\partial y}\right)^2\\
& -2ia_j\left(k_{xj}\frac{\partial}{\partial x} + k_{yj}\frac{\partial}{\partial y}\right) - a_j\left(\frac{\partial^2}{\partial x^2} + \frac{\partial^2}{\partial y^2}\right)
\end{aligned} \tag{2.5}$$

https://doi.org/10.1017/S0022377897006193 Published online by Cambridge University Press

and

$$V_{k_ik_jk_l} = ik_{yj}(\boldsymbol{k}_j \times \boldsymbol{k}_i)\cdot \boldsymbol{e}_{||}(k_j^2 - k_i^2)V,$$
$$a_j = k_{yj}^2[-u_j(\eta_i + \tfrac{16}{3}\varepsilon_n) + 10\varepsilon_n + 8\eta_i - 2],$$
$$V = 2\varepsilon_n - \tfrac{2}{3} - \tfrac{1}{4}\eta_i, \quad u_j = \frac{\omega_j}{k_{yj}}.$$

The $\pm$ signs before the first term in (2.5) correspond to the two branches of the linear η_i modes (2.2).

Sufficiently far from the boundary of marginal stability or for sufficiently small wave amplitudes, when the opposite inequality to (1.1) is satisfied, the system (2.4) describes conventional explosive instability. For our problem, this is valid if

$$\tau_{nl}(\omega_k^+ - \omega_k^-) \gg 1 \quad \text{or} \quad \tau_{nl}\varepsilon_n^{1/2}(\eta_{icr}^0 - \eta_i) \gg 1.$$

The temporal development of this instability for η_i modes has been considered before in Nordman *et al.* (1993). In the present paper we consider explosive instability in the other limiting case:

$$\tau_{nl}(\omega_k^+ - \omega_k^-) \ll 1 \quad \text{or} \quad \tau_{nl}\varepsilon_n^{1/2}(\eta_{icr}^0 - \eta_i) \ll 1,$$

when the inequalities (1.1) hold.

3. Temporal development of explosive instability near the boundary of marginal stability

Near the boundary of marginal stability, the temporal evolution of nonlinear instability is described by

$$\frac{d^2\chi_j}{dt^2} = W_{k_jk_lk_m}\chi_l^*\chi_m^*, \tag{3.1}$$

where $\chi_j = i\Phi_{k_j}$, and the matrix elements $W_{k_jk_lk_m} = iV_{k_jk_lk_m}$ are real. The indices j, l and m run through the values (1,2,3), (2,3,1) and (3,1,2) respectively.

The system has self-similar 'explosive' solutions for equal signs of the matrix elements (Davydova 1982; Davydova and Zmudskii 1994):

$$\chi_i = \frac{6}{(|W_{k_jk_ik_l}W_{k_ik_jk_l}|)^{1/2}\,(t_0 - t)^2}. \tag{3.2}$$

For different signs of the matrix elements ($\mathrm{sign}(W_{k_1k_2k_3}) = -\mathrm{sign}(W_{k_2k_3k_1}) = -\mathrm{sign}(W_{k_3k_2k_1})$) (Davydova and Zmudskii 1994),

$$\chi_1 = \frac{2\sqrt{21}\exp(i\alpha)}{(|W_{k_2k_3k_1}W_{k_3k_2k_1}|)^{1/2}\,(t_0 - t)^{2(1-i\sqrt{3})}},$$
$$\chi_2 = \chi_3\left(\left|\frac{W_{k_2k_3k_1}}{W_{k_3k_2k_1}}\right|\right)^{1/2} = \frac{2\sqrt{42}\exp(i\beta)}{(|W_{k_3k_2k_1}W_{k_1k_2k_3}|)^{1/2}\,(t_0 - t)^{2-i\sqrt{3}}}, \tag{3.3}$$

where α and β are constants.

Except for the 'explosive' solutions, the system (3.1), with different signs of the matrix elements, also has solutions (Fig. 1*a*) with one growing mode fitted approximately to $\chi_1 \propto at^{4/3}$ and two decaying oscillating modes fitted to $\chi_2, \chi_3 \propto (\frac{8}{3}a)^{1/2}t^{-1/3}\cos(\frac{3}{5}a^{1/2}t^{5/3} + \theta_0)$, where a and θ_0 are constants. In the general case

https://doi.org/10.1017/S0022377897006193 Published online by Cambridge University Press

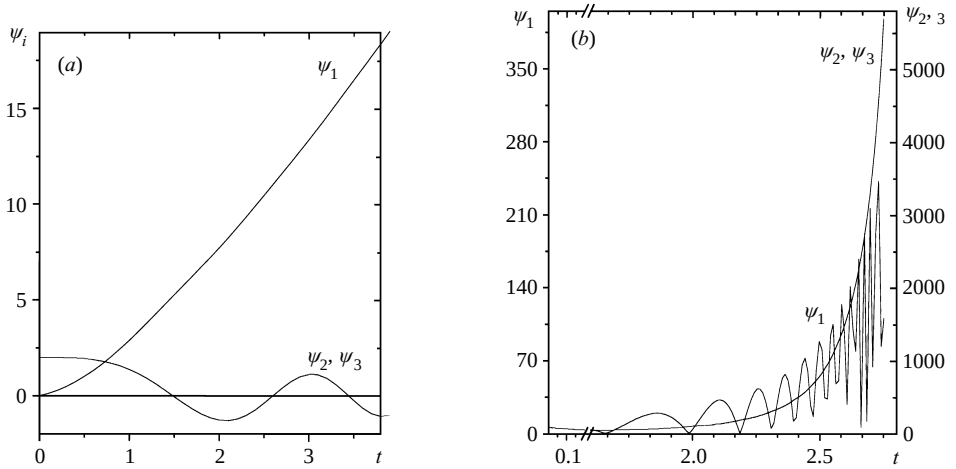


Figure 1. Amplitudes of η_i modes $\chi_j = \psi_j \exp(i\varphi_j)$ near the boundary of marginal stability as the solution of the system (3.1) under the initial conditions: (*a*) $\psi_1(0) = \psi'_{2,3}(0) = 0$, $\psi'_1(0) = 1$, $\psi_{2,3}(0) = 2$, $\varphi_i(0) = \varphi'_i(0) = 0$; (*b*) $\psi_1(0) = 6$, $\psi_{2,3}(0) = 8.49$, $\psi'_1(0) = -12$, $\psi'_{2,3}(0) = -16.97$, $\varphi_1(0) = -0.05$, $\varphi_{2,3}(0) = 0.5$, $\varphi'_1(0) = -2$, $\varphi'_{2,3}(0) = 1$.

of the system (3.1), the solution (Fig. 1*b*) consists of a combination of 'explosive' and 'non-explosive' solutions.

The arbitrary solution of the system (3.1) with equal signs of the matrix elements tends to the self-similar solution (3.2). The solutions (3.2) and (3.3) describe modified explosive instability when all three interacting waves are 'zero-energy waves'. The amplitudes of all modes during an explosive instability increase simultaneously owing to the source of the non-equilibrium of the medium. In our case this is an inhomogeneity of background plasma parameters.

4. Modified explosive instability saturation in a bounded domain

Temporal description of instability is valid only if one can consider interacting waves with amplitudes that does not depend on the space coordinates. In reality, this is not the case, and we should solve the spatial–temporal problem to describe the wave-amplitude evolution. In this case an obvious generalization of the system (3.1) that follows from (2.4) is

$$\left(\frac{\partial}{\partial t} - u_j \frac{\partial}{\partial x}\right)^2 \chi_j = V_{k_j k_l k_m} \chi_l^* \chi_m^*. \tag{4.1}$$

First let us consider the simplified case of equal and real wave amplitudes $\chi_j = \chi$, equal phase velocities $u_j = u$ and equal signs of the matrix elements. Then the system (4.1) reduces to the equation

$$\left(\frac{\partial}{\partial t} - u \frac{\partial}{\partial x}\right)^2 \chi = \chi^2. \tag{4.2}$$

Here the amplitudes are renormalized so that $V_{k_j k_l k_m} = 1$. Introducing a new function $\chi^{-1/2}$ and then using the Laplace time transform, it can be shown that

https://doi.org/10.1017/S0022377897006193 Published online by Cambridge University Press

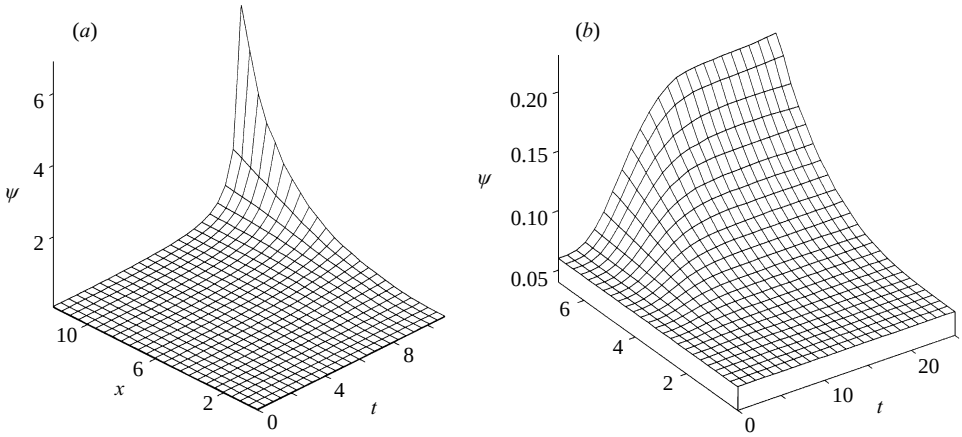


Figure 2. Two alternatives for the system (4.1), depending on the relative magnitudes of the system length L and the 'explosive' length L_{expl} ($\psi_i\,|_{t=0,x} = \psi_i|_{t,x=0} = 0.06$, $\partial\psi_i/\partial t\,|_{t=0,x} = \partial\psi_i/\partial x|_{t,x=0} = 4 \times 10^{-6}$, $\varphi_1\,|_{t=0,x} = \varphi_1|_{t,x=0} = 1$, $\varphi_2\,|_{t=0,x} = \varphi_2|_{t,x=0} = 2$, $\varphi_3\,|_{t=0,x} = \varphi_3|_{t,x=0} = 0.5$, $\partial\varphi_i/\partial t\,|_{t=0,x} = \partial\varphi_i/\partial x|_{t,x=0} = 0$, $u_1 = 1$, $u_2 = 1.05$, $u_3 = 0.95$, $t_{expl} \approx 13.5$, $L_{expl} \approx 12.8$): (*a*) explosion ($L > L_{\text{expl}}$); (*b*) saturation ($L < L_{\text{expl}}$).

(4.2) has the following solution in the interval $0 \leqslant x \leqslant L$:

$$\chi(x,t) = \begin{cases} \dfrac{6}{(t_0 - t)^2}, & \left(0 \leqslant t < \dfrac{x}{u}, \quad t < \left(\dfrac{6}{a}\right)^{1/2} = t_0\right), \\ \dfrac{6u^2}{(l_0 - x)^2}, & \left(t > \dfrac{x}{u}, \quad x < \left(\dfrac{6}{b}\right)^{1/2} u = l_0\right) \end{cases} \tag{4.3}$$

for the initial and boundary condition $\chi(x,0) = a$ and $\chi(0,t) = b$, with $a < b$. Hence for $t > L/u$ a steady state on the interval L is established in the nonlinear system (4.2) if $L < l_0 < t_0 u$, where l_0 is an 'explosive length' of the instability for the corresponding 'spatial' problem of the system (4.1). The steady state describes a spatial distribution of amplitude corresponding to the finite spatial amplification. We have found numerically for other boundary and initial conditions that, during the temporal evolution of the instability, different initial amplitudes tend to become equal and the phase difference $\varphi_1 - \varphi_2 - \varphi_3$ tends to zero as $t \to t_0$. Numerical calculations confirm that for given boundary conditions at $x = 0$ on the finite interval $(0, L)$ a steady state is established in a time $L/\min(u_j)$ if L is less than the 'explosive length' l_0. We have checked this conclusion numerically for a wide spectrum of initial and boundary conditions and for any signs of the matrix elements $V_{k_j k_l k_m}$, as well as for different signs of u_j (see the example in Fig. 2). Figure 2(*a*) demonstrates explosive instability in the case $L > l_0$. Figure 2(*b*) corresponds to the case $L < l_0$, when a steady state is established after a time $L/\min(u_j)$.

The model (4.1) may be applied to nonlinear wave interactions near the boundary of marginal stability in various non-equilibrium systems. One such system is a plasma with a monoenergetic ion beam (Dum and Ott 1971). This system becomes linearly unstable if the velocity of the ion beam u is less than the sound velocity c_s, or more strictly if $u < c_s(1 + \eta)^3$, where $\eta = n_b/n \ll 1$ (n and n_b are the den-

https://doi.org/10.1017/S0022377897006193 Published online by Cambridge University Press

sities of the plasma and the ion beam respectively). If $u \gtrsim c_s\,(1+\eta)^3$, the system is near the boundary of marginal stability. In the experiment of Nakamura *et al.* (1980) two probe waves were injected into a plasma–ion-beam system, and the third eigenmode was excited so that the matching conditions (2.3) were fulfilled. Simultaneous amplitude growth of all three waves was detected, which is characteristic of explosive instability. This instability was interpreted by Davydova (1982) as the explosive instability of 'zero-energy waves'. It explains adequately the observed characteristic time scales of temporal waves evolution.

Studies of the interaction between two electromagnetic waves and a relativistic electron beam in a free-electron laser (Davydova *et al.* 1987) give an example of the development of explosive instability in a bounded domain.

Although the considerations above are evidently too simplified for η_i modes in tokamaks, they demonstrate that inhomogeneity may play the role of a stabilizing factor, leading to the formation of a steady state.

5. Envelope soliton solutions

5.1. The case of homogeneous background parameters

In this subsection we seek steady solutions of the full system (2.4). We consider the possibility of localized solutions (envelope solitons) moving with constant velocity U along the direction of drift-wave propagation ($\widehat{\boldsymbol{y}}$). To do this, we introduce a new variable $\xi = y + Ut$ and assume that the envelope soliton has the form

$$\chi_j = \psi_j(\xi) e^{i\left(s_j y + q_j x\right)}, \tag{5.1}$$

with parameters $s_j \ll k_{yj}$ and $q_j \ll k_{xj}$, which satisfy the conditions

$$s_1 + s_2 + s_3 = 0, \tag{5.2}$$

$$q_1 + q_2 + q_3 = 0. \tag{5.3}$$

Then the real functions ψ_j satisfy the following set of ordinary differential equations:

$$\left[1 + \frac{(U-u_j)^2}{a_j}\right] \frac{d^2\psi_j}{d\xi^2} - 2i\left[\frac{u_j(U-u_j)s_j}{a_j} + \frac{k_{yj}\delta_j(U-u_j)}{2a_j} + k_{yj} - s_j\right] \frac{d\psi_j}{d\xi} - \left(\frac{u_j^2 s_j^2}{a_j} - 2k_{xj}q_j - 2k_{yj}s_j\right)\psi_j = \frac{V_{k_j k_l k_m}}{a_j}\psi_l\psi_m. \tag{5.4}$$

On putting the second coefficient in the system (5.4) equal to zero, we arrive at the set of equations

$$s_j\left[1 - \frac{u_j(U-u_j)}{a_j}\right] = k_{yj}\left[1 + \frac{1}{2}\frac{\delta_j}{a_j}(U-u_j)\right] \approx k_{yj}, \tag{5.5}$$

which, along with the condition (5.2), determines two possible soliton velocities $U^{\pm}$:

$$U^{\pm} \approx \frac{k_{y1}^3\,(V_2+V_3) + k_{y2}^3\,(V_1+V_3) + k_{y3}^3\,(V_2+V_1) \pm D^{1/2}}{2(k_{y1}^3 + k_{y2}^3 + k_{y3}^3)}, \tag{5.6}$$

https://doi.org/10.1017/S0022377897006193 Published online by Cambridge University Press

where $V_j \approx u_j + a_j/u_j$ and

$$D = [k_{y1}^3 (V_2 - V_3) + k_{y2}^3 (V_3 - V_1) + k_{y3}^3 (V_1 - V_2)]^2 + 4k_{y2}^3 k_{y3}^3 (V_1 - V_2)(V_1 - V_3).$$

Then one can find the parameters s_j from (5.5).

One can see that $D > 0$ and $U^{\pm}$ are real in all instances. The soliton velocities $U^{\pm}$ are of the order of the phase velocity of drift waves. Next, we denote

$$\lambda_j = \frac{2k_{xj}q_j + 2k_{yj}s_j - u_j^2 s_j^2/a_j}{1 + (U - u_j)^2/a_j}, \tag{5.7}$$

As a result, after the renormalization

$$\psi_j = -\frac{\phi_j (a_l a_m)^{1/2}}{(|W_{k_l k_m k_j} W_{k_m k_j k_l}|)^{1/2}},$$

the system (5.4) takes the simple form

$$\frac{d^2\phi_j}{d\xi^2} + \lambda_j \phi_j + S_j \phi_l \phi_m = 0, \tag{5.8}$$

where $S_j = \mathrm{sign}(W_{k_j k_l k_m})$. So far, the soliton parameters q_j are still arbitrary.

There are two principally different cases, depending on the signs of the matrix elements.

If all the signs are equal ($S_1 = S_2 = S_3 = 1$) and all the parameters λ_j are equal,

$$\lambda_1 = \lambda_2 = \lambda_3 = -\lambda^2, \tag{5.9}$$

then the system (5.8) has a particular analytical solution in the form of a KdV soliton:

$$\phi_1 = \phi_2 = \phi_3 = \frac{3\lambda^2}{2\cosh^2[\frac{1}{2}\lambda (y + Ut - y_0)]}. \tag{5.10}$$

Similar types of solitons have been found by Nozaki *et al.* (1979) in a simpler drift-wave model described by the Hasegawa–Mima equation in the presence of a non-uniform DC electric field.

Otherwise, when the signs of the matrix elements are different ($-S_1 = S_2 = S_3 = 1$) and the parameters λ_j are related as

$$-\lambda_1 = \tfrac{1}{2}\lambda_2 = \tfrac{1}{2}\lambda_3 = -\lambda^2 \tag{5.11}$$

then the system (5.8) has a soliton solution in the form

$$\phi_1 = 6\lambda^2 \frac{\sinh[\lambda (y + Ut - y_0)]}{\cosh^2[\lambda (y + Ut - y_0)]}, \tag{5.12a}$$

$$\phi_{2,3} = -\frac{3\lambda^2}{\cosh^2[\lambda (y + Ut - y_0)]}. \tag{5.12b}$$

The soliton parameters q_j and λ in both cases (5.10) and (5.12) are determined from (5.3) complemented by three additional conditions for λ_j, (5.9) or (5.11). For the solution (5.12), the soliton intensity $|\phi_1|^2$ of the first mode has two bumps, in contrast to the two other drift-soliton envelopes $|\phi_2|$ and $|\phi_3|$. Soliton solutions of the system (5.8) with arbitrary values of q_j (and hence λ_j) can be found numerically. In Fig. 3 an example of the numerical solution of the system (5.8) with unequal values

https://doi.org/10.1017/S0022377897006193 Published online by Cambridge University Press

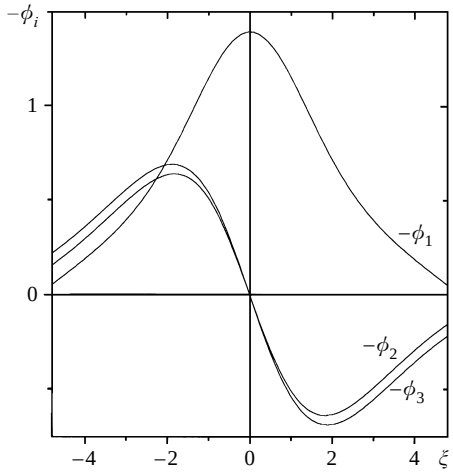


Figure 3. Soliton solution of the system (5.8) with $\lambda_1 = -0.4$, $\lambda_2 = 0.25$ and $\lambda_3 = 0.35$

of λ_j is presented. This case is similar to the case (5.11), considered analytically. The numerical simulation confirms that soliton solutions with two bumps are typical for the system (5.8) with different signs of λ_j.

Thus, for fixed coefficients of the system (5.4), envelope drift solitons may propagate with two different velocities (5.6). A similar property holds for small-amplitude linear η_i modes: two eigenmodes (2.2) with the same wave vector propagate with different phase and group velocities. In the process of nonlinear interaction, they 'merge' into a 'zero-energy wave', but the double nature of the latter wave manifests itself after self-saturation. This feature is likely to be inherent to non-linear evolution of 'zero-energy' or reactively unstable modes. For example, two nonlinear localized wave structures are formed in the nonlinear self-stabilizing stage of electron-beam–plasma instability. Such structures have been observed experimentally by Yamagiwa *et al.* (1989) to move with slightly different velocities of order of the group velocity v_g of the most-unstable linear mode ($v_g = \frac{2}{3}v_0$, where v_0 is the electron-beam velocity). This experiment was interpreted theoretically by Davydova and Lashkin (1992).

5.2. The case of inhomogeneous background parameters

Up to now, we have supposed that all the background parameters of our model nonlinear system (all coefficients) are homogeneous. In the general case, two-dimensional inhomogeneity of the magnetic tokamak field is of great importance for the formation of structure elements of turbulence. Linear localized ITG structures, so-called ballooning ITG modes, are formed in a tokamak magnetic field (Romanelli and Zonca 1993; Taylor *et al.* 1996). Short-scale structures are usually described in the strong-ballooning approximation. The width of these structures in the poloidal direction is determined by a Schrödinger-equation eigenproblem with square potential well ($U(\theta) = U_0(\theta_0) - \kappa(\theta_0)(\theta - \theta_0)^2$, where θ_0 is an extremum of the effective potential function). The deepest potential well is usually formed at the outer part of the discharge ($\theta_0 = 0$ and $\kappa(\theta_0) = 0$), leading to the ballooning nature of linear global drift modes. Experiments and simulations indicate that the characteristic size of structures cannot be explained only by linear effects (Weiland 1994). As

https://doi.org/10.1017/S0022377897006193 Published online by Cambridge University Press

we have shown in the previous subsection, nonlinear coupling may lead to localized structure formation even in the case of homogeneous background parameters. The influence of both linear effects, or the existence of an effective potential well determined by the tokamak magnetic field geometry, and nonlinear wave–wave interaction effects on ITG structures is of great interest. In particular, we try to elucidate whether localized drift structures may be formed on the inner side of the torus ($\theta_0 = \pi$ and $\kappa(\theta_0) < 0$) due to nonlinear coupling. In this subsection we use the nonlinear system (5.8), taking into account the dependence of the parameters λ_j on the poloidal ($\widehat{\boldsymbol{y}}$) direction near the extremum points ($\lambda_j \to \lambda_j + \kappa_j y^2$):

$$\frac{d^2\chi_j}{d\xi^2} + (\lambda_j + \kappa_j\xi^2)\chi_j + S_j\chi_l\chi_m = 0, \tag{5.13}$$

where χ_j is connected with the drift-wave potentials Φ_{k_j} by $\chi_j = i\Phi_{k_j}$ and $\xi = y + Ut$. Here we assume that the envelopes of interacting drift-mode potentials χ_j are localized near the point $y = 0$ where the parabolic approximation for the dependence of λ_j on y is valid.

In the linear approximation, three equations of the system (5.13) are independent. A simple analysis (Romanelli and Zonca 1993) shows that in this case a well-localized mode in the $\widehat{\boldsymbol{y}}$ direction may exist for negative κ_j and positive discrete eigenvalues λ_j. In the case of positive κ_j the corresponding linear problem (5.13) was interpreted by Romanelli and Zonca (1993) as describing extended modes escaping from the point $y = 0$ in both directions with imaginary eigenvalues λ_j. However, nonlinear wave coupling can essentially change this picture. We have shown that the system (5.13) admits stationary localized solutions both for $\kappa_j > 0$ and for $\kappa_j < 0$. The results of numerical simulations (Fig. 4) reveal that two possible types of nonlinear structure can appear in such a system. In contrast to the case of a linearized system, a monotonically decaying localized solution (Fig. 4*a*) has been found for parameters $\kappa_j < 0$ and $\lambda_j < 0$. An envelope soliton solution with oscillating tails (Fig. 4*b*) corresponds to the case ($\kappa_j > 0$), when the linearized system (5.13) has no localized solution either.

6. Discussion

We have shown that near the boundary of marginal stability, nonlinear explosive instability of ITG driven modes develops even if the plasma is linearly stable. The instability may result in coherent η_i structures that constitute the structure of subcritical turbulence. An explanation of subcritical plasma turbulence and anomalous transport was advanced by Yagi *et al.* (1996) and Itoh et al. (1996) on the basis of an MHD model of the electrostatic current diffusive intercharge mode. In their 'self-sustained turbulence' theory, the nonlinear marginal stability condition determines the anomalous transport coefficient. They stressed the nonlinear instability as a governing factor for anomalous transport. However, in contrast to our approach, they supposed that excited modes are completely decorrelated and uniformly distributed in space. Then the self-stabilization of the instability occurs because of enhanced transport. We believe that the turbulent state arises after the saturation of the instability and the appearance of the coherent structures. The turbulent state is formed in interactions (collisions) of these structures. Some numerical 2D simulations confirm this point of view (Ottaviani *et al.* 1990). The contribution of

https://doi.org/10.1017/S0022377897006193 Published online by Cambridge University Press

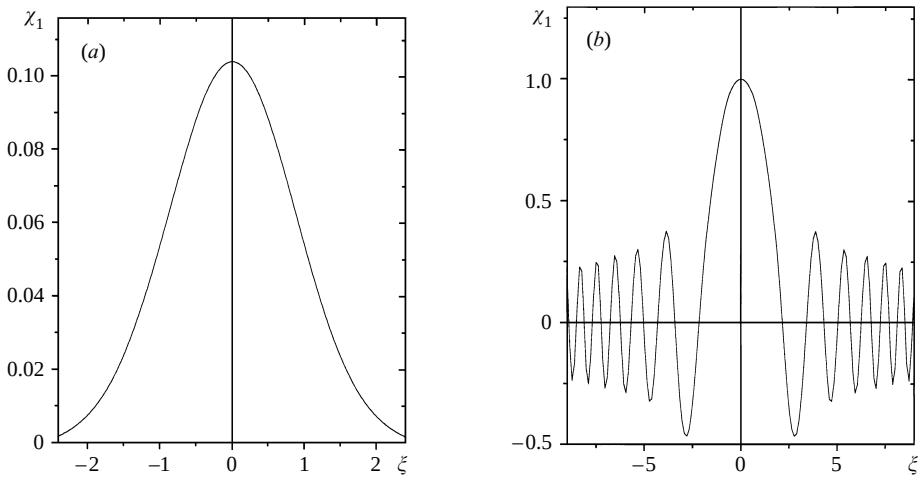


Figure 4. Amplitude of the first η_i mode as a solution of the system (5.13) under the following conditions: (*a*) $\lambda_{1,2} = -1.26$, $\lambda_3 = -1.17$, $\kappa_1 = -1.7$, $\kappa_2 = -2.3$, $\kappa_3 = -1.44$, $V_j = 1$; (*b*) $\lambda_1 = 1.2$, $\lambda_2 = 1$, $\lambda_3 = 0.8$, $\kappa_1 = 0.9$, $\kappa_2 = 5$, $\kappa_3 = 1.1$, $V_j = 1$.

dipole vortices to anomalous transport was considered by Horton and Hasegawa (1994) and Nycander and Isichenko (1990).

In the framework of a simple three-wave interaction model, we have shown that the formation of spatially non-uniform structures is a plausible saturation mechanism for nonlinear instabilities. It may happen that these structures turn out to be unstable against perpendicular perturbations, as is the case for the one-dimensional drift solitons discovered by Oraevskii *et al.* (1969). Petviashvili (1977) has shown that this instability leads to stable monopolar two-dimensional drift-soliton or vortex formation in the case of a scalar nonlinearity. Such vortices have been observed in model experiments on water in rotating vessels and in the Earth's magnetosphere (Pokhotelov *et al.* 1996). We expect that two-dimensional ITG structures are also formed near the boundary of marginal stability. This assumption is supported by Ottaviani *et al.* (1990) in numerical simulations of a similar nonlinear system describing ITG two-dimensional structure formation in the nonlinear stage of instability, where the nonlinear instability associated with the existence of a non-positive-definite energy invariant develops. The Hamiltonian of the system describing modified explosive instability of zero-energy modes is also non-positive-definite (Davydova 1982; Davydova and Zmudskii 1994). We believe that our considerations clarify the mechanisms leading to drift-structure formation near the boundary of marginal stability.

References

Andersson, P. and Weiland, J. 1988 *Phys. Fluids* **31**, 359.
Biglary, H., Diamond, P. H. and Rosenbluth, M. N. 1989 *Phys. Fluids* **B1**, 109.
Connor, J. W. 1995 *Plasma Phys. Contr. Fusion* **37**, A119.
Coppi, B. 1980 *Comments Plasma Phys. Contr. Fusion* **5**, 261.
Dauchot, O. and Daviaud, F. 1995 *Phys. Fluids* **A7**, 901.
Davydova, T. A. 1982 *Proceedings of International Conference on Plasma Physics, Göteborg* (ed. H. Wilhelmsson), p. 192.

https://doi.org/10.1017/S0022377897006193 Published online by Cambridge University Press

Davydova, T. A. 1984 *Nonlinear and Turbulent Processes in Physics* (ed. R. Z. Sagdeev), Vol. 1, p. 177. Harwood, New York.
Davydova, T. A. and Lashkin, V. M. 1992 *Ukrainskii Fiz. Zh.* **37**, 1833 (in Russian).
Davydova, T. A. and Oraevskii, V. N. 1974 *Zh. Eksp. Teor. Fiz.* **66**, 1032 (in Russian).
Davydova, T. A. and Zmudskii, A. A. 1994 *Plasma Phys. Rep.* **20**, 723.
Davydova, T. A., Pavlenko, V. P., Taranov, V. B. and Shamrai, K. P. 1976 *Phys. Lett.* **59A**, 91.
Davydova, T. A., Zakharov, V. P. and Kulish, V. V. 1987 *Soviet J. Tech. Phys.* **32**, 418.
Dum, C. T. and Ott, E. 1971 *Plasma Phys.* **13**, 177.
Guzdar, P. N., Chen, L., Tang, W. M. and Rutherford, P. H. 1983 *Phys. Fluids* **26**, 673.
Hahm, T. S. and Tang, W. M. 1989 *Phys. Fluids* **B1**, 1185.
Horton, W. and Hasegawa, A. 1994 *Chaos* **4**, 227.
Horton, W., Choi, D. I. and Tang, W. M. 1981 *Phys. Fluids* **24**, 1077.
Horton, W., Su, K. N. and Morrison, P. J. 1990 *Soviet J. Plasma Phys.* **16**, 562.
Itoh, K., Itoh, S.-I., Fukuyama, A. and Yagi, M. 1996 *Plasma Phys. Rep.* **22**, 721.
Kishimoto, Y., Tajima, T., Horton, W., LeBrun, M. J. and Kim, J.-Y. 1996 *Phys. Plasmas* **3**, 1289.
Kurki-Suonio, T. K., Groebner, R. J. and Burrell, K. H. 1992 *Nucl. Fusion* **32**, 133.
Moiseev, S. S., Pungin, V. G., Sagdeev, R. Z., Suyazov, A. V. and Yanovskii, V. V. 1983 *Nolineynye Volny*, p. 85. Nauka, Moscow (in Russian).
Mordovskaya, V. G. and Oraevskii, V. N. 1985 *Fiz. Plazmy* **11**, 1350.
Nakamura, S., Yuyma, T., Kubo, H. and Mitani, K. 1980 *J. Phys. Soc. Japan* **48**, 2112.
Nordman, H. and Weiland, J. 1989 *Nucl. Fusion* **29**, 251.
Nordman, H., Pavlenko, V. P. and Weiland, J. 1993 *Phys. Fluids* **B5**, 402.
Nozaki, K., Taniuti, T. and Watanabe, K. 1979 *J. Phys. Soc. Japan* **46**, 983.
Nycander, I. and Isichenko, M. B. 1990 *Phys. Fluids* **B2**, 2042.
Oraevskii, V. N., Tasso, H. and Wobig, H. 1969 *Plasma Physics and Controlled Nuclear Fusion Research*, Vol. 1, p. 671. IAEA, Vienna.
Ottaviani, M., Romanelli, F. and Benzi, R. 1990 *Phys. Fluids* **B2**, 67.
Pavlenko, V. and Weiland, J. 1993 *Physica Scripta* **47**, 96.
Petviashvili, V. I. 1977 *Soviet J. Plasma Phys.* **3**, 151.
Pokhotelov, O. A., Stenflo, L. and Shukla P. K. 1996 *Plasma Phys. Rep.* **22**, 941.
Rewoldt, G., Tang, W. M. and Hastie R. J. 1987 *Phys. Fluids* **30**, 807.
Riccardi, C., Gamterale, L., Salierno, M. and Fontanesi, M. 1996 *Proceedings of International Conference on Plasma Physics, Nagoya, Abstracts*, 12 A09, 228.
Romanelli, F. 1989 *Phys. Fluids* **B1**, 1018.
Romanelli, F. and Zonca, F. 1993 *Phys. Fluids* **B5,** 4081.
Romanelli F., Tang W. H. and White R. B. 1986 *Nucl. Fusion* **26**, 1515.
Shukla, P. K. and Weiland, J. 1989 *Phys. Rev.* **A40**, 341.
Taylor, J. B., Wilson, H. R. and Connor, J. W. 1996 *Plasma Phys. Contr. Fusion* **38,** 243.
Terry, P. W., Leboeuf. J. N., Diamond, P. H., Thayer, D. R., Sedlak, J. E. and Lee, G. S. 1988 *Phys. Fluids* **31**, 2920.
Walts, R. S. 1985 *Phys. Rev. Lett.* **55**, 1098.
Weiland, J. 1994 *Current Top. Phys. Fluids* **1**, 439.
Yagi, M., Itoh, S. I., Itoh, K., Fukuyama, A. and Azumi, M. 1995 *Phys. Plasmas* **2**, 4140.
Yamagiwa, K., Tokuda, K. and Mieno, T. 1989 *Proceedings of International Conference on Plasma Physics, New Delhi, Contributed Papers* (ed. A. Sen and P. K. Kaw), Vol. 3, p. 1021.

https://doi.org/10.1017/S0022377897006193 Published online by Cambridge University Press